eNeuro

Testosterone or estradiol when implanted in the medial preoptic nucleus trigger short low-amplitude songs in female canaries

Laura M. Vandries[1], Samar Ghorbanpoor[1], Gilles Cornez[1], Olesya Shevchouk[1], Gregory F. Ball[2], Charlotte A. Cornil[1] and Jacques Balthazart[1]

[1]GIGA Neurosciences, University of Liege, Liège, Belgium
[2]Department of Psychology, University of Maryland, College Park, MD 20742

1 **Second revision on March 31st**
2
3 **Testosterone or estradiol when implanted in the medial preoptic nucleus**
4 **trigger short low-amplitude songs in female canaries**
5
6
7 **Abbreviated Title:** Preoptic testosterone activates female song
8
9
10 Laura M. Vandries[1], Samar Ghorbanpoor[1], Gilles Cornez[1], Olesya Shevchouk[1],
11 Gregory F. Ball[2], Charlotte A. Cornil[1] and Jacques Balthazart[1]
12
13 [1] *GIGA Neurosciences, University of Liege, Liège, Belgium*
14 [2] *Department of Psychology, University of Maryland, College Park, MD 20742*
15
16 **Author Contributions:**
17 GFB, CAC and JB Designed Research; LMV, SG,GC and OT Performed Research;
18 GFB, CAC and JB Wrote the paper
19
20
21 **Key words:** song control system; medial preoptic nucleus, singing motivation;
22 songbirds, POM, testosterone, estradiol
23
24
25 Number of Figures   9
26 Number of Tables   1
27 Number of Multimedia   0
28 Number of words for Abstract   249
29 Number of words for Significance Statement   119
30 Number of words for Introduction   641
31 Number of words for Discussion   2303
32
33
34 **Conflict of Interest**   Authors report no conflict of interest
35
41
42
43
44 Corresponding author
45 Jacques Balthazart: GIGA Neurosciences, University of Liege, 15 avenue Hippocrate,
46 B-4000 Liège, Belgium
47 Phone: +32 4 366 59 70 ---Fax: +32 4 366 59 71 --- e-mail: jbalthazart@ulg.ac.be
48

49

Abstract

In male songbirds, the motivation to sing is largely regulated by testosterone action in the medial preoptic area, whereas testosterone acts on song control nuclei to modulate aspects of song quality. Stereotaxic implantation of testosterone in the medial preoptic nucleus (POM) of castrated male canaries activates a high rate of singing activity, albeit with a longer latency than after systemic testosterone treatment. Systemic testosterone also increases the occurrence of male-like song in female canaries. We hypothesized that this effect is also mediated by testosterone action in the POM. Females were stereotaxically implanted with either testosterone or with estradiol targeted at the POM and their singing activity was recorded daily during 2 hours for 28 days until brains were collected for histological analyses. Following identification of implant localizations, 3 groups of subjects were constituted that had either testosterone or estradiol implanted in the POM or had an implant that had missed the POM (Out). Testosterone and estradiol in POM significantly increased the number of songs produced and the percentage of time spent singing as compared with the Out group. The songs produced were in general of a short duration and of poor quality. This effect was not associated with an increase in HVC volume as observed in males, but testosterone in POM enhanced neurogenesis in HVC, as reflected by an increased density of doublecortin-immunoreactive multipolar neurons. These data indicate that, in female canaries, testosterone acting in the POM plays a significant role in hormone-induced increases in the motivation to sing.

71

72

73

74

Highlights

- Testosterone implantation in the preoptic area activates singing in female canaries

- A similar activation is induced by estradiol in the preoptic area

- Songs produced tend to be short and of poor quality

- Testosterone also increases neurogenesis in HVC

- Observed changes in neurogenesis are likely activity-dependent

Significance

Systemic testosterone increases male-like song in adult female canaries. We demonstrate by stereotaxic implantation of testosterone or estradiol that this effect is mediated, as has been demonstrated in males, by hormone action in the preoptic area. These implants significantly increased the number of songs produced and the percentage of time spent singing, but the songs produced remained short in duration and simple in structure. This singing activity did not result in an increase in HVC volume, as observed in males, but there was an enhanced density of doublecortin-immunoreactive new neurons supporting the notion that HVC neurogenesis is at least in part activity–dependent. These data also indicate that neural mechanisms regulating testosterone-induced singing are similar in males and females.

94

95

Introduction

Male song produced by songbirds (members of the suborder Passeres or oscines) functions to promote territory defense and to attract female mates (Catchpole and Slater, 2008; Collins, 2004). Male song is therefore often produced, especially among species in the temperate zone, at its highest rates and in its most stereotypic fashion during the breeding season (Catchpole and Slater, 2008; Schlinger and Brenowitz, 2017). Both the high rate of singing and the high degree of stereotypy are facilitated by testosterone (T) acting in males at brain targets via androgenic and estrogenic metabolites (Harding, 2008; Schlinger and Brenowitz, 2017).

In male canaries specifically, there is clear evidence that song rate and quality and the morphology of the song system are regulated by seasonal changes in T (Nottebohm et al., 1986; Nottebohm et al., 1987). Androgenic and estrogenic metabolites of T seem to be involved in these processes (Fusani and Gahr, 2006; Fusani et al., 2003). The effects of T on these different components of song production are mediated by T acting in distinct areas of the brain (Alward et al., 2017b). T in the preoptic area is important for effects on song rate (Alward et al., 2013), while T acting on nuclei in the song control system, such as HVC or the robust nucleus of the arcopallium (RA), is important for effects on song stereotypy (Alward et al., 2017a; Alward et al., 2016).

Female songbirds also sing in some species and, although there is evidence that female song is actually an ancestral feature in the passerine order (Odom et al., 2014), much less is known about the function and neuroendocrine control of female song (e.g., (Odom and Benedict, 2018)). The specialized neural circuit regulating song tends to contain brain nuclei of larger volume in males than in females, even in

120   species where females sing at a higher or similar rate than males (Ball, 2016; Gahr et

121   al., 2008). However, there is a rough relationship between brain variation and sex

122   differences in behavior in that the sex difference in song nuclei volumes tends to be

123   more robust in species with little or no female song as compared to species where

124   females produce substantial song (Ball et al., 2008; MacDougall-Shackleton and Ball,

125   1999). The role of hormones in adult song production in females and where they

126   might act is however not well understood.

127   Female canaries only sing very infrequently very short primitive songs and

128   correlatively the volume of their song control nuclei is 2 to 5 times smaller than in

129   males (Nottebohm and Arnold, 1976). Interestingly, treating adult female canaries

130   with male-typical concentrations of T does increase the volume of their song control

131   nuclei and makes their song more male-like in rate and complexity (Hartog et al.,

132   2009; Nottebohm, 1980), though this sex difference in brain and behavior can not be

133   completely reversed based on adult hormone treatment (Madison et al., 2015).

134   The ability of exogenous T to stimulate more male-like song in adult female

135   canaries provides an opportunity to study where and how hormones can act in the

136   female brain to regulate song production, a male-typical behavior. Specifically, we

137   employed here stereotaxic procedures to ask whether T or its estrogenic metabolite,

138   17β-estradiol (E2), act in the preoptic area of female canaries to regulate song rate.

139   These females were compared to females which also had received a T or E2 brain

140   implant, but in which the implant had missed its intended target (the preoptic area)

141   and was therefore presumably unable to activate singing behavior. We show that in

142   females the medial preoptic area plays a key role in the control of the singing

143   motivation as has been shown in males. This study also demonstrates that activating

144   singing results in an increased neurogenesis in the telencephalic song control area

145 HVC, which brings additional support to the idea that this neurogenesis is at least in

146 part activity-dependent.

147

148 **Materials and methods**

149

150 *Subjects and experimental procedures*

151 This experiment was performed on a total of 32 adult female canaries (*Serinus*

152 *canaria*) of the Fife fancy breed that were obtained as adults from a breeding colony

153 established at the University of Antwerp, Belgium. Birds were kept on a short day

154 photoperiod (8L:16D) between their arrival in the laboratory and the beginning of the

155 experiment. At that time females were isolated in one of our 16 custom-built sound-

156 attenuated boxes and their vocal behavior was recorded for 2 hours in the morning

157 for two days to ensure that they were not singing.

158 Sound was acquired from all 16 channels simultaneously via custom-made

159 microphones (microphone from Projects Unlimited/Audio Products Division, amplifier

160 from Maxim Integrated) and an Allen & Heath ICE-16 multichannel recorder. The

161 sound file was acquired and saved as a .wav file by Raven v1.4 software

162 (Bioacoustics Research Program 2011; Raven Pro: Interactive Sound Analysis

163 Software, Version 1.4, Ithaca, NY: The Cornell Lab of Ornithology) at a sampling

164 frequency of 44,100 Hertz.

165 During the next two days each female received a stereotaxic implant of

166 testosterone (T) or estradiol-17β (E2) aimed at the medial preoptic nucleus (POM).

167 Brain implants were prepared, filled with crystalline testosterone or crystalline E2 and

168 implanted into the POM following a previously published procedure (Alward et al.,

169 2013). Briefly, implants were prepared using blunted 27 gauge needles filled over a

length of 1 mm with crystalline T or E2. Under isoflurane anesthesia subjects were fixed in a stereotaxic apparatus with ear bars and a beak holder holding the head in a standardized position. The following stereotaxic coordinates were used to target the POM: dorsoventral: −6.5 mm from the dorsal surface of the brain; anterior–posterior: 2.2 mm from the rostral tip of the cerebellum; and medio–lateral: ± 0.15 mm from midline. Half of the subjects in each group were implanted on the left side of the brain and half on the right side.

The skull immediately over these coordinates was removed with a micro-drill, the implant was lowered to the targeted position, dental cement was applied around the implant and the skin was sutured. The bird was placed under a heat lamp to recover until perching. Birds were returned to their sound-attenuated box where photoperiod was switched to 16L:8D to photostimulate the birds mimicking a reproductive state (Hurley et al., 2008) and their vocalizations were then recorded for 30 days during two hours daily immediately following lights-on (0900h).

There were 16 recording boxes available for this experiment which was therefore run in two successive cohorts with the exact same procedure. In the first cohort all 16 females were implanted with testosterone to test specifically the effect of this steroid, but one died soon thereafter. Since positive results had been obtained with T, the second cohort was mostly used to test the effects of E2. 12 females were thus implanted with E2, but four females received T to provide an internal control between cohorts. We did not treat additional subjects with empty implants because it was anticipated that in a substantial number of birds the implant targeted to the POM would actually miss its target, so that these subjects could be used as negative controls. Previous work in canaries indeed showed that empty implants and T-filled

194 implants that miss their target produce similar behavioral results (Alward et al., 2013;

195 Alward et al., 2016).

196   All experimental procedures complied with Belgian laws concerning the

197 Protection and Welfare of Animals and the Protection of Experimental Animals, and

198 experimental protocols were approved by the Ethics Committee for the Use of

199 Animals of the University of Liege (Protocol number 1739). In all housing situations

200 food, water, baths, cuttlebone and grit were available ad libitum.

201

202   ***Brain collection and sectioning***

203 Canaries were deeply anesthetized with 0.04 mL of Nembutal. Once reflexes had

204 stopped, birds were perfused through the heart with phosphate-buffered saline (PBS,

205 1.43 g/L Na_2HPO_4, 0.48 g/L KH_2PO4, 7.2 g/L NaCl) until return flow in the atrium was

206 clear, followed by 4% paraformaldehyde (Sigma) in PBS 0.1M. Brains were dissected

207 out of the skull and post-fixed overnight in the same fixative solution. The syrinx and

208 ovary were extracted and weighed, and the cloacal protuberance (length x width)

209 was measured. On the next day, brains were rinsed in PBS and transferred to 30%

210 sucrose in PBS stored at 4°C until they sank. They were then frozen on dry ice and

211 stored at -80°C until used.

212   Brains were notched on the left side, then cut into 4 series of 30 μm-thick

213 coronal sections with a Leica CM 3050S cryostat. The sections were collected in Tris

214 buffered-saline (TBS; 0.05 M Tris, 0.9% NaCl, pH 7.6). Sections were stored in a

215 cryoprotective solution (0.01M PBS with 10 g/L polyvinylpyrrolidone, 300 g/L sucrose,

216 and 300 ml/L ethylene glycol) and stored at -20°C until used.

217

218   ***Nissl staining***

219   The first series of sections was mounted on Superfrost™ slides and left to dry

220   overnight. After rehydration in baths of decreasing concentrations of isopropanol,

221   slides were stained with toluidine blue and differentiated in Walpole buffer and

222   molybdate buffer. The sections were then dehydrated in increasing concentrations of

223   isopropanol and lastly in xylene and coverslipped with Eukitt™ mounting medium

224   (Sigma). These sections were later used to identify the implants location and to

225   determine HVC volumes.

226

227   ***DCX immunohistochemistry***

228   The second series of brain sections was stained by immunohistochemistry for

229   doublecortin (DCX), a marker of young new neurons in the canary HVC (Balthazart

230   and Ball, 2014; Balthazart et al., 2008), to quantify neurogenesis in HVC and its

231   periphery and obtain a second independent measure of HVC volume by techniques

232   previously described and validated for canaries (Alward et al., 2014; Balthazart et al.,

233   2008; Boseret et al., 2007; Shevchouk et al., 2017a; Yamamura et al., 2011). Briefly,

234   sections were sequentially rinsed 3 X 5 min in TBS, 15 min in H_2O_2 3% in TBS, 3 X 5

235   min in TBS and 30 min in blocking solution containing 1% bovine serum albumin

236   (BSA), 5% normal goat serum (NGS), 0.1% triton X in TBS. Sections were then

237   incubated in primary antibody raised in rabbit against doublecortin (Abcam ab18723;

238   1/2000 in TBS-T i.e., TBS containing 0.1% triton-X and 1% BSA) for one hour at

239   room temperature and then 48h at 4°C on a rotating shaker. Sections were washed 3

240   X 5 min in TBS and incubated for 2 hours in the secondary antibody solution

241   (biotinylated goat anti-rabbit antibody; Jackson Immunoresearch 1/500 in TBS-T) at

242   room temperature still on a rotating shaker. Sections were rinsed 3 X 5 min in TBS

243   and incubated in the biotin-avidin complex (ABC; 1/400 Vector Elite Kit, Vector

244 Laboratories). The antigen-antibody complexes were finally visualized with the use of
245 a SG substrate kit for peroxidase (Vector laboratories). Tissues were then mounted
246 on microscope slides, dried and coverslipped with Eukitt™ mounting medium
247 (Sigma).

248

249 **Aromatase immunohistochemistry**

250 Sections from the third series were separated in two pools containing tissue from the
251 telencephalon or from the diencephalon-brain stem. The telencephalon sections were
252 immunostained for parvalbumin and chondroitin sulfate to label perineuronal nets
253 (see next section). Diencephalic-brain stem sections were immunostained for
254 aromatase by methods previously described and validated (Balthazart et al., 1996;
255 Balthazart et al., 1997; Foidart et al., 1995; Shevchouk et al., 2017b).

256 Briefly, sections were rinsed 3 X 5 min in TBS, 20 min in H_2O_2 0.6% in TBS, 3
257 X 5 min in TBS and 1 hour in blocking solution containing 1% BSA, 5% NGS and
258 0.2% triton X in TBS. Sections were incubated in primary antibody raised in rabbit
259 against aromatase (a generous gift of Dr. N. Harada Toyoake, Japan; 1/10,000 in
260 TBS-T 0.2% triton-X 1% BSA) for one hour at room temperature followed by an
261 overnight incubation at 4°C on a rotating shaker. Sections were then washed 3 X 5
262 min in TBS, blocked in a solution containing 1% BSA and 5% NGS and 0.2% triton X
263 in TBS and incubated for 2 hours in biotinylated goat anti-rabbit antibody (Jackson
264 Immunoresearch, 1/200 in TBS with 0.2% triton-X, 1% BSA and 5% NGS) at room
265 temperature on a rotating shaker. Sections were rinsed 3 X 5 min in TBS and
266 incubated in the biotin-avidin complex ABC (1/400 Vector Elite Kit, Vector
267 Laboratories). The binding sites were finally visualized by a 10 min incubation in
268 0.04% 3,3'-diaminobenzidine (DAB) with 0.012% H_2O_2 diluted in TBS. Sections were

269 mounted onto glass slides, dried overnight, immersed in xylene for 10 min and

270 coverslipped with Eukitt™ mounting medium (Sigma).

271

272 ***Parvalbumin and chondroitin sulfate staining***

273 The telencephalic tissue from the 3rd series of sections was then simultaneously

274 immunostained for parvalbumin (PV) and chondroitin sulfate to label perineuronal

275 nets (PNN) as described previously (Cornez et al., 2018b; Cornez et al., 2017b;

276 Cornez et al., 2015) to obtain an additional measure of HVC plasticity (van 't Spijker

277 and Kwok, 2017). Sections were rinsed 3 X 5 min in TBS and incubated in blocking

278 solution made of 5% NGS and 0.1% triton X in TBS. Sections were then incubated

279 overnight in a mixture of two primary antibodies including a polyclonal rabbit raised

280 against parvalbumin (Abcam ab11427; 1/1000 in TBS-T 0.1% triton-X) and a

281 monoclonal mouse anti-chondroitin sulfate antibody (1/500 in TBS-T 0.1% triton-X,

282 Sigma-Aldrich C8035) for 48 h at 4°C on a rotating shaker. On the next day, sections

283 were then washed 3 X 5 min in TBS and incubated for 2 h at room temperature on a

284 rotating shaker in a cocktail of secondary fluorescent antibodies containing goat anti-

285 mouse Alexa Fluor 488 (1/100, Invitrogen) and goat anti-rabbit Alexa Fluor 546

286 (1/200, Invitrogen). Sections were rinsed 3 X 5 min in TBS and then mounted on

287 glass slides. Sections were dried and coverslipped with Vectashield™ mounting

288 medium containing DAPI (4',6-Diamidine-2'-phenylindole dihydrochloride) to label all

289 cell nuclei.

290

291 ***Microscopy and image analysis***

292   All quantitative analyses were performed on both sides of the brain and are

293   presented separately taking into account whether the area under study was on the

294   ipsi- or contra-lateral side with respect to the implant targeting the POM.

295

296   *Implant localization*

297   The exact location of implant tips relative to the POM was checked in each subject by

298   identifying the implant track and its end in the series of sections stained for Nissl

299   material or immunostained for aromatase, which defines the boundaries of POM and

300   adjacent bed nucleus of the stria terminalis (BNST) in quail (Charlier et al., 2008) and

301   has been previously used as a marker of POM in canaries (Shevchouk et al., 2017b;

302   Shevchouk et al., 2018b). These locations were then plotted on semi-schematic

303   drawings of the canary brain derived from the published atlas (Stokes et al., 1974)

304   where the location of the aromatase-immunoreactive (ARO-ir) cells was added

305   based on previous immunohistochemical work on canaries (Metzdorf et al., 1999;

306   Shevchouk et al., 2017b) and zebra finches (Balthazart et al., 1996; Balthazart et al.,

307   1997; Saldanha et al., 2000).

308

309   *POM volumes*

310   All sections stained for aromatase that contained the medial preoptic nucleus (POM)

311   in both the right and left hemispheres were photographed at 10X magnification with

312   the Leica Application Suite 4.5.0 and a camera connected to a Leica DMRB FL 100

313   microscope using the same light settings for all pictures. A line was drawn around the

314   cluster of the ARO-ir cells defining the POM identified on all sections starting from the

315   most rostral section containing ARO-ir cells at the level of the tractus

316   septopalliomesencephalicus to the most caudal section at the level of the anterior

317 commissure. The area defined by this line (in μm^2) was calculated with the area

318 measurement function of the ImageJ software (Wayne Rasband, National Institutes

319 of Health) and then the volume of the POM on each brain side was calculated by

320 adding all areas and multiplying the sum by 120 μm i.e., is the distance between two

321 successive sections in the same series.

322

323 *HVC volumes*

324 Photomicrographs were taken at 5X magnification of each Nissl-stained section

325 containing HVC in both hemispheres with the same camera and microscope. HVC

326 boundaries were drawn and its surface in each section was determined with ImageJ.

327 These areas were added and the volume of the nucleus was obtained by multiplying

328 this sum by 120 μm. These calculations were separately performed for both sides of

329 the brain.

330 Given that HVC boundaries could also be determined by the dense cluster of

331 DCX-ir neurons present in the nucleus, the boundaries and volume of HVC were also

332 determined based on the sections stained for DCX by the same procedure on

333 microphotographs taken at 10X magnification.

334

335 *Neurogenesis and DCX quantification*

336 In each hemisphere, cells labeled for DCX were counted in the entire HVC in all

337 sections containing this nucleus that were used to compute the volume of the

338 nucleus. DCX-positive cells were also counted in each of these sections in a 400 μm

339 X 800 μm rectangle (0.32 mm^2) placed at the ventral edge of HVC and another

340 similar rectangle placed just lateral to HVC. These counts were performed on

341 photomicrographs acquired at 5 X magnification with the camera and microscope

342 described before. The two types of DCX cells (see (Balthazart et al., 2008; Boseret et

343 al., 2007) were counted separately: the fusiform cells that presumably are very young

344 neurons still migrating and the more or less round multipolar cells that are slightly

345 older neurons that have initiated their final differentiation. The sums of these counts

346 of cells (fusiform and multipolar) in each location (in HVC, ventral and lateral to HVC)

347 were computed separately and divided by the surface that had been counted to

348 derive densities of positive cells per mm^2.

349

350   *PV-PNN quantification*

351 Four separate sets of photomicrographs of HVC were obtained in each bird on the

352 left and right side in fluorescent light at 40X magnification with a Leica DMRB FL 100

353 microscope, selecting in each case the 4 sections where HVC had the largest area.

354 Within each set, 3 photomicrographs were obtained with the 3 different filters

355 allowing the visualization of the Alexa Fluor 488 (green for PNN), the Alexa Fluor 546

356 (Red for parvalbumin) and of DAPI (blue). Within each field (0.043 mm^2) that had

357 been photographed, we counted with ImageJ the number of parvalbumin-positive

358 cells and the number of perineuronal nets surrounding at least half the outline of a

359 cell body. We additionally merged the green (PNN) and red (PV) photomicrographs

360 to quantify the number of PNN that were surrounding PV-positive cells. We also

361 merged the green (PNN) and blue (DAPI) photomicrographs to confirm that those

362 PNN that were not around a PV cell were actually surrounding another type of cell.

363 These counts were averaged across the 4 sections for each hemisphere of each bird,

364 which allowed us to determine the density of PV-immunoreactive cells, of PNN, and

365 of PNN surrounding PV-ir cells (PNN+PV) per mm^2. This procedure also allowed us

366   to compute the percentage of PV cells surrounded by PNN and vice versa the

367   percentage of PNN that were located around PV cells.

368

369   ***Song Analysis***

370   Songs recorded from all subjects for 2 hours on days 7, 14 and 28 after placement of

371   the brain implants were analyzed with the Raven Pro 1.5 software. Females only

372   rarely produced long songs lasting several seconds as males typically do. Female

373   vocalizations in most cases consisted of just a few syllables produced in rapid

374   succession. Single syllables and very short vocalizations were very frequent and it

375   was decided to ignore them for the present study given that they were observed with

376   a high degree of frequency before the beginning of the steroid treatments. Instead,

377   we focused on vocalizations lasting at least 0.4 s, separated by at least 0.4 s of

378   silence. These vocalizations were manually selected on the sound spectrograms

379   generated by Raven and then the program calculated a number of measures of these

380   vocalizations including the song duration, maximum frequency, 90% bandwidth, and

381   average Wiener entropy.

382   The entropy measure is an indicator of the width and uniformity of the power

383   spectrum. It can be thought of as a measure of disorder in a sound, as a pure tone

384   has in this context an entropy equal to zero, while higher entropy values correspond

385   to greater disorder in a sound, as white noise would have an entropy value of 1. The

386   average entropy reported here corresponds to the mean of all values of entropy

387   measured for each section of the recording corresponding to songs (See

388   http://www.birds.cornell.edu/brp/raven/RavenFeatures.html for the description of all

389   these measurements). From the number of songs and their duration, we additionally

390   computed the percentage of time that birds were singing during the recordings.

391

Statistics

All data associated with a single measure per subject were analyzed as appropriate by Student t-tests or one-way analyses of variance (ANOVA) with experimental groups as an independent variable. When multiple data (measures on different days or on different brain locations) were available, they were analyzed by two-way General Linear Model (GLM) mixed-effect analyses. All calculations were made with GraphPad Prism V8 software on MacIntosh

HVC volumes measured in sections stained for Nissl material or for DCX were compared by the Pearson product moment correlation coefficient.

Effects were considered significant for $p < 0.05$. All data are presented by their mean ± SEM. Morphological or histological data from a few birds and song recordings from one subject were accidentally lost during processing resulting in a slightly smaller number of subjects for some analyses. The number of available data points is indicated in each case at the bottom of the corresponding bar in the figures.

406

Results

408

Implant location

Due to poor perfusion, the brain from one subject could not be used. Therefore we were able to collect neuroanatomical data for 30 females, 18 that had been implanted with T (8 in the left, 10 in the right hemisphere) and 12 implanted with E2 (5 in the left, 7 in the right hemisphere).

Inspection of the implants tracks and tips in the Nissl-stained sections and in sections stained for aromatase revealed that out of the 18 T-implanted females, 14 (7

416   on the left, 7 on the right side) had the tip of their implant located in the ARO-ir cell

417   group defining the POM, while 4 were outside the nucleus. In the E2-implanted

418   females, 7 (1 on the left, 6 on the right side; including one located at the very caudal

419   end of the nucleus, see Fig. 1D) had the tip of their implant in the POM, while 5 had

420   their implant outside the nucleus.

421

422   Insert figure 1 about here

423

424   *Data reduction*

425   In order to summarize data, we first considered whether the side of T implantation

426   (left vs. right) had any impact on the results. The number of songs produced on days

427   7, 14 and 28 were not affected (p=0.652, p=0.564 and p=0.659 respectively).

428   Similarly, we tested potential effects of the side of T implantation on all brain

429   measures collected on both sides by two-way GLM mixed-effect analysis utilizing the

430   side of implantation as an independent variable and the side of measures as a

431   repeated factor. For the measures considered (POM volume, HVC volume in DCX or

432   Nissl-stained sections, densities of multipolar and fusiform DCX-ir neurons in, ventral

433   or lateral to HVC, density of PNN, of PV-ir cells, of PV+PNN and percentage of PNN

434   with PV in HVC), these analyses did not reveal significant effects of the side of

435   implantation or of its interaction with the side of brain for all measures considered,

436   with only two exceptions.

437   The analysis of POM volumes identified a significant interaction between side

438   of implantation and the brain measure (p<0.001) but no overall effect of implantation

439   side (p=0.251) or side of measure (p=0.695). The volume of this nucleus was larger

440   on the implantation side and this will be discussed in the corresponding place in the

441   results section. In addition, analysis of the DCX-ir cells in HVC detected a significant

442   effect of the side of implantation for multipolar cells (p=0.006). This difference reflects

443   a larger number of multipolar cells on both sides of the brain when implants were

444   placed in the right POM compared to the left POM. This suggests that, for some

445   unexplained reason, newborn neurons had multiplied and matured more rapidly in

446   the group of females implanted with T on the right side. These effects will be taken

447   into account in the following results sections, however, given the overall negative

448   results obtained here, all subsequent analyses will only consider the pooled data as a

449   function of whether they were collected on the ispi- or contra-lateral side with respect

450   to the steroid implant irrespective of whether implants were on the left or right side.

451   A similar analysis of effects of implant side was impossible for E2-implanted

452   birds since only a single subject ended up having a cannula implanted in the left

453   POM. Other cannulae aimed at the POM ended up outside the nucleus. The two

454   groups of subjects were therefore pooled in this case as in the previous case.

455   In a second step we considered whether T-filled (n=4) and E2-filled (n=5)

456   implants that ended up outside the POM had a different impact on brain and behavior.

457   All these implants were in a position dorso-lateral to the POM and ventral to the tip of

458   the lateral ventricle (see Fig. 1). We compared all data for these two groups of Out

459   birds by two-way GLM mixed-effect analysis with one independent factor, the two

460   groups, and one repeated measure, the different days of recording or the two brain

461   sides. Table 1 reports the mean ± SEM and the number of observations for each

462   separate set of Out data, and the results of all these ANOVAs. In every single case,

463   non-significant (p≥0.05) probabilities were detected.

464   Insert table 1 about here

465

466   Therefore in the rest of this presentation all results are analyzed after being

467   pooled in 3 experimental groups: birds with T in POM (T group; n=14), E2 in POM

468   (E2 group; n=7) and birds with T or E2 outside of POM (Out group; n=9)

469

470   *Morphological data*

471   At the end of the experiment, the body mass of the 3 groups of females was very

472   similar (Fig 2A; $F_{2,30}$=0.478, p=0.625). The cloacal protrusion, a marker of androgen

473   action (Luine et al., 1980; Tramontin et al., 2000) was on average slightly increased

474   in the T group and decreased in the E2 group by comparison with the control Out

475   group (Fig. 2B) but the effect was not statistically significant ($F_{2,20}$=2.875, p=0.080).

476   Surprisingly syrinx mass differed between groups (Fig. 2C; $F_{2,28}$= 3.516, p=0.043)

477   with the T group being significantly smaller (p=0.034) than the Out group (p=0.034).

478   This effect might however only result from a poor (too large) dissection in two

479   subjects of the Out group that were clearly outliers (25.5 and 26.2 mg versus a

480   mean±SD of 14.21±2.15 after their exclusion). If these 2 values are excluded

481   (hatched bar in Fig. 2C) there is no longer an effect of treatments on syrinx weight

482   ($F_{2,28}$= 1.109, p=0.345). Ovary mass was also not affected by the treatments (Fig. 2

483   D; $F_{2,28}$= 0.471, p=0.629).

484

485   Insert figure 2 about here

486

487   *Singing behavior*

488   Most females were at the beginning of the experiment producing short vocalizations

489   including only one or two syllables that lasted only 0.2 to 0.4 seconds. Within 7 days

490   after implantation of T or E2, these vocalizations became more frequent and they

491 increased based both on duration and on the number of different syllables present

492 within a song. The maximal rate of production was observed on day 14 in the T group

493 and on day 28 in the E2 group. Figure 3 illustrates the type of songs that were

494 produced by T or E2 treated females with implants in POM as well as by a female

495 with an implant that missed its target.

496

497 Insert figure 3 about here

498

499 The visual inspection of all sonograms indicated that, as illustrated in figure 3,

500 there was a large variation in the duration and structure of these songs. Some lasted

501 a very short time and consisted of the repetition of a single syllable; others had

502 multiple syllable types that were repeated for durations up to 6-7 seconds. This

503 variability is reflected in the large variability of durations illustrated in Figure 4B.

504

505 Insert figure 4 about here

506

507 All songs identified during the 2 hour recording sessions that occurred on days

508 7, 14 and 28 of the experiment were quantitatively evaluated with the Raven Pro

509 software and results were analyzed by two-way GLM mixed-effect analysis with the 3

510 different groups and 3 recording times as independent and repeated factors

511 respectively. The number of songs produced (Fig. 4A) significantly varied over time

512 ($F_{1.95, 52.64}=4.304$, $p=0.019$) and these changes were different in the 3 groups as

513 revealed by a significant interaction between time and groups ($F_{4,54}=2.780$, $p=0.036$).

514 The overall group difference was however not statistically significant ($F_{2,27}=2.760$,

515 $p=0.081$). Comparisons of the T and E2 groups to the Out group by the Tukey test

indicated significant differences between T and Out and between E2 and Out on days 14 and 28.

The average duration of individual songs (Fig. 4B) slightly increased over time and did so on average more prominently in the T and E2 groups but analysis of these data indicated no significant effect of time ($F_{1.15,27.12}=0.717$, p=0.424), no group difference and no interaction ($F_{2,26}=0.797$, p=0.461 and $F_{4,47}=0.685$, p=0.606 respectively).

The percentage of time that birds were singing during the two hours recordings (Fig. 4C) that reflects both the numbers of songs and their duration also increased over time although the effect was not fully significant ($F_{1.94,52.30}=3.087$, p=0.056). There was however a significant overall group difference ($F_{2,27}=3.924$, p=0.032) and an interaction between groups and time ($F_{4,54}=3.192$, p=0.020). Tukey multiple comparisons tests confirmed the presence of significant differences between T and Out and between E2 and Out on days 14 and 28 day 28.

A more detailed analysis of the songs sampled focused on 3 additional parameters: the song maximum frequency, the 90% bandwidth, and the average entropy. Analyses of these measures by mixed-effects model (birds that were not singing on a given day could not be assigned a value) revealed no group difference (p≥ 0.317) and no interaction (p≥0.291). A moderate time effect was observed for the analysis of the maximum frequency ($F_{1.49,34.47}=3.759$, p=0.045), but not for the two other measures. Yet, since it is not associated with an interaction, this effect cannot result from the steroid treatments. Post-hoc tests indicated that the song maximal frequency was significantly higher on day 28 than on day 7.

POM Volume

541   The volume of the POM as defined by the dense group of ARO-ir neurons was

542   analyzed by a two-way GLM mixed-effect analysis with the three groups as

543   independent factors and the two sides of the brain (ipsi- and contra-lateral to the

544   implant) as a repeated factor. This analysis revealed a significant effect of the brain

545   side ($F_{1,23}$=16.87, p<0.001) and interaction between groups and side of the brain

546   ($F_{2,23}$=8.241, p=0.002) but no overall effect of treatments ($F_{2,23}$=1,921, p=0.169; Fig

547   5A). The Tukey multiple comparisons tests indicated that POM volume was larger on

548   the implantation side in the T group compared to both the E2 and Out group but

549   these differences was not present on the contralateral side.

550

551   Insert figure 5 about here

552

553   Insert figure 6 about here

554

555   *HVC Volume*

556   HVC volume was assessed both in Nissl-stained sections and in sections

557   stained for DCX that highlights the boundaries of HVC based on the higher density of

558   DCX-ir cells inside as compared to outside the nucleus. The two-way GLM mixed-

559   effect analysis identified no effect of treatment (Nissl: $F_{2,25}$=0.574, p=0.571; DCX:

560    $F_{2,27}$=0.672, p=0.519), no difference between ipsi- and contra-lateral sides (Nissl:

561    $F_{1,25}$=0.042, p=0.838; DCX: $F_{1,27}$=0.182, p=0.673) and no interaction between these

562   factors (Nissl: $F_{2,25}$=0.912, p=0.415; DCX: $F_{2,27}$=0.788, p=0.465).

563   Interestingly, the volumes of HVC as measured in Nissl or DCX-ir stained

564   sections were significantly correlated both on the ipsi and contra lateral sides, even if

-22-

565 this correlation was not perfect (see Figure 7; ipsi: r=0.520, p=0.005; contra: r=0.717,

566 p<0.001).

567

568   Insert figure 7 about here

569

570   *Neurogenesis (DCX)*

571 Despite the absence of global effect of the treatments on the volume of HVC, we

572 asked whether steroids implanted in POM had affected the rate of neurogenesis in

573 this nucleus. Fusiform and multipolar DCX-ir cells were therefore quantified

574 separately in HVC and, as a control, in two equivalent areas, one just ventral and one

575 just lateral to the nucleus (Figure 8).

576   Two-way GLM mixed-effect analysis of the number of DCX-ir cells in HVC (3

577 treatments as independent factor and two sides, ipsi vs. contra lateral, as repeated

578 factor) identified a statistical trend suggesting an effect of the treatments on fusiform

579 (fusiform: $F_{2,27}$=2.527, p=0.099**)** and a significant effect of treatments on multipolar

580 ($F_{2,27}$=3.658, p=0.039) DCX-ir cells (Fig. 8A-B). There was no effect of brain side

581 (fusiform: $F_{1,27}$=1.208, p=0.281; multipolar: $F_{1,27}$=0.737, p=0.399**)** and no interaction

582 between brain side and treatment (fusiform: $F_{2,27}$=0.825, p=0.449; multipolar:

583 $F_{2,27}$=0.024, p= 0.976). The overall treatment effect of multipolar cells was associated

584 in the Tukey post hoc tests with a significant difference between the T and E2 group

585 (p=0.049) but the T vs. Out difference failed to reach statistical significance (p=0.164).

586   Note that in the data reduction section, we had noticed that females with a T

587 implant in the right POM had more multipolar DCX-ir cells in HVC. Given however

588 that identical numbers of birds had an implant in the left and in the right POM this

589 difference based on side of implantation has no impact on the results presented here.

590   There was actually no average difference in numbers of cells between the ipsi- and

591   contralateral sides of the brain with respect to the implant.

592   Similar analyses of DCX-ir cells densities counted in an equivalent area just

593   ventral or just lateral to HVC (Fig. 8C-F) identified no effect of treatments ($p \geq 0.141$),

594   of the side of the brain ($p \geq 0.273$) and of their interaction ($p \geq 0.672$, except for the

595   multipolar DCX-ir cells in ventral position where $p=0.070$ but this effect does not

596   seem to be associated with an interpretable effect of the steroids; detailed statistics

597   not shown).

598

599   Insert figure 8 about here

600

601   *Perineuronal nets*

602   This experiment was also providing an occasion to probe the mechanisms underlying

603   the testosterone-induced expression of PNN in the song control system. Previous

604   work in male canaries demonstrated that systemic treatment with exogenous

605   testosterone increases the density of PNN in HVC (Cornez et al., 2017a). Given that

606   this treatment simultaneously activated an intense singing activity, it was impossible

607   in this situation to determine whether the increased PNN expression results from a

608   direct action of testosterone on HVC or indirectly from the increased neuronal activity

609   in this nucleus. Females receiving a testosterone implant in POM potentially allowed

610   us to discriminate between these two possibilities.

611

612   Insert figure 9 about here

613

614   The density of PNN (number per mm^2) in HVC was not affected by the

615   treatments ($F_{2,26}=0.947$, p=0.401), side of the brain ($F_{1,26}=0.489$, p=0.490) or their

616   interaction ($F_{2,26}=2,678$, p=0.087; Figure 9A). Since most PNN form around PV-

617   positive cells, this type of cells was also quantified but this identified no significant

618   effect (treatments: $F_{2,26}=1.301$, p=0.289; side: $F_{1,26}=1.285$, p=0.267; interaction:

619     $F_{2,26}=0.019$, p=0.980). The density of PV-positive cells associated to PNN was

620   similarly not affected (treatments: $F_{2,52}=0.203$, p=0.817; side: $F_{1,52}=0.438$, p=0.511;

621   interaction: $F_{2,52}=0.895$, p=0.415) and this was also the case of the percentage of

622   PNN associated with PV cells (treatments: $F_{2,52}=0.260$ p=0.778; side: $F_{1,52}=0.051$,

623   p=0.821; interaction: $F_{2,52}=1.844$, p=0.168).

624

625   **Discussion**

626   This experiment demonstrates that, as shown previously in males (Alward et al.,

627   2013; Alward et al., 2016), implantation of testosterone in the medial preoptic nucleus

628   (POM) increases vocal production in female canaries. This behavioral effect was

629   accompanied by changes in aromatase expression in the POM and also by a

630   bilateral increase in neurogenesis in HVC. No change in PNN expression, which is

631   usually associated with song crystallization in both canaries and zebra finches, was

632   however observed in HVC. Because effects of testosterone on singing are thought to

633   be induced at least in part by the action of its estrogenic metabolites at the cellular

634   level (Fusani and Gahr, 2006; Fusani et al., 2003), we also implanted some females

635   with estradiol (E2) in the POM and demonstrate that this resulted in relatively similar

636   behavioral effects, but there were no statistically significant effects when one

637   examined the neural measures. No significant difference between treatment groups

638   could be detected in body mass, the size of the cloacal protrusion (an androgen-

639   dependent structure), the mass of the syrinx (androgen-dependent also) or of the

640   ovary. The syrinx mass in particular was roughly similar to what was previously

641   observed in females that are not systemically treated with sex steroids (Shevchouk et

642   al., 2017b). These data suggest that there was little or no leakage of steroids from

643   the brain implants to the periphery and at any rate that this leakage was not

644   differential between the 3 groups of subjects and thus cannot explain differences

645   among treatment groups. This conclusion is also supported by the observation that T

646   implants increased POM volume on the ipsi- but not on the contra-lateral side of the

647   brain, indicating that steroid diffusion did not even reach his adjacent location. These

648   results allow us to draw a number of general conclusions but also raise a number of

649   questions that need to be considered.

650

651   *Singing Activity*

652   In the large number of subjects that received a T or E2 implant in the POM, a clear

653   increase in singing activity was detected. This was reflected in the production of a

654   larger number of vocalizations and, in some subjects, an increase in their duration,

655   but this latter effect was too variable to be significant. The percentage of time spent

656   singing that reflects both the number and duration of these vocalizations was also

657   markedly increased by both T and E2 implants, when located in the POM as

658   compared to birds in which the implant had missed its target.

659   Post-hoc tests indicated that a significant effect of T acting in the POM on

660   singing behavior was observed earlier after treatment than for E2 (day 14 versus 28),

661   while the reverse would be expected if all effects of T are mediated after its

662   conversion to E2. This observation could thus support the idea that T itself is

663   implicated in the activation of singing, but the average difference between these two

664   groups was small and could simply reflect slightly different localizations of the

665   implants, a differential diffusion of the steroid in brain tissue or even the lower

666   statistical power of the experiment for the E2 group (7 E2 in POM vs. 14 T in POM

667   females).

668   The quality of the songs produced by these females remained very poor as

669   compared to male-typical songs. Their average duration barely increased, with only a

670   few females producing songs lasting longer than one and even more rarely two

671   seconds. No significant effect of treatments on maximum frequency, bandwidth,

672   entropy, or average entropy could be observed. This pattern corresponds to a large

673   extent to what was observed in males, where implantation of T in the POM increased

674   the song rate, but did not modify the quality of the vocalizations (Alward et al., 2013;

675   Alward et al., 2016).

676   Songs in females with T or E2 in POM were however of much poorer quality

677   than in similarly treated males. Average song duration in males with T in POM was

678   indeed around 4 seconds (Alward et al., 2013), while it barely reached 0.6 seconds in

679   females. Furthermore, female songs usually consisted of the repetition of 2 or 3

680   syllables that were not fully crystallized (no sharp definition in sonograms, variability

681   from one rendition to the next), while more diversity in syllable usage was observed

682   in males with T in POM even if a large degree of variability between successive

683   renditions was also present.

684   Overall, the female songs observed here had a distribution of energy that

685   showed a higher degree of general disorder than fully crystallized male songs. In two

686   independent unpublished experiments performed in our laboratory on the same

687   breed of canaries, we indeed observed that the average entropy of male songs in the

688   spring is around 2.5, while entropy measured here was equal to or greater than 3

689   (Cornez et al. 2018a; Cornez and Balthazart, unpublished data).

690   The origins of these sex differences in response to hormone treatment are

691   difficult to identify at this stage. It is however likely that it reflects a rather fundamental

692   difference between males and females since even when treated systemically with T

693   for 3 weeks males and females still sing songs that are qualitatively different

694   (Madison et al., 2015). It is unlikely that the difference between songs observed here

695   in females and those previously observed in similarly treated males (Alward et al.,

696   2013; Alward et al., 2016) simply reflects a difference in hormonal activation. The

697   size and position of implants used here are indeed similar to those used and

698   observed in the male experiments. One possible reason for this difference is that the

699   females receiving these POM implants have not experienced as robust a process of

700   sensory-motor song learning as the males experienced. It is known that female

701   songbirds can learn to recognize the songs of their conspecific males (Catchpole and

702   Slater 2008; Gentner and Hulse, 2000; Nowicki and Searcy, 2014). However, it is

703   reasonable to assume that the hormonal activation of song in an individual who has

704   robustly experienced sensory-motor learning would be less effective than in an

705   individual who has. This sex difference could of course also reflect more fundamental

706   genetic sex differences related to song production in canaries, but this could only be

707   determined by ontogenetic experiments investigating the development of song in

708   males and females exposed to identical endocrine conditions.

709   It should also be noted that a number of song features significantly changed

710   over the course of the experiment, but in a similar manner in the three groups of

711   subjects (no effect of treatments and no interaction of time with treatment). This is the

712   case for the maximum frequency and the three measures of song amplitude

713   (maximum, peak and RMS) that are not reported here. These changes presumably

714   reflect the transfer from short to long days (from 8 to 16 hours of light per day) of the

715   birds at the beginning of the experimental phase that should have promoted a limited

716   increase in ovarian activity and consequently in circulating E2 concentrations.

717

718   *The POM as identified by aromatase immunohistochemistry*

719   The position of implants was mapped in sections stained for Nissl material but also

720   stained by immunohistochemistry for aromatase, which provides a clearer and easier

721   identification of the POM. It was shown previously that a systemic treatment with T

722   increases within a few days aromatase expression and the related POM volume as

723   assessed by the dense cluster of ARO-ir cells in female (Shevchouk et al., 2017b)

724   and male (Shevchouk et al., 2018a) canaries.

725   A significantly larger volume of the ARO-ir cell group defining POM was

726   observed here on the side ipsilateral to the brain implant in the T group, but a similar

727   effect was not observed after implantation of E2. This increase specifically observed

728   in the ispilateral side of T birds confirms the local efficacy of the steroid implants in

729   the present design and, as already mentioned, their action limited to the immediate

730   surrounding of the implant tip. It has previously been shown in several avian species

731   that E2 largely mimics the effects of T in the induction of aromatase (Harada et al.,

732   1993; Hutchison et al., 1989; Hutchison and Steimer, 1986). Why this was not the

733   case here remains unexplained and can only be ascribed at this point to the dose or

734   diffusion of the steroid.

735

736   *HVC volume and neurogenesis*

737   It was previously observed that unilateral implantation of T in the POM of males

738   significantly increases HVC volume on both sides of the brain (Alward et al., 2013;

739   Alward et al., 2016), but this effect was not replicated here in females. Volumes

740   measured both in Nissl-stained sections and based on the dense DCX-ir cell group

741   identified no treatment effect and no treatment by side interaction, although these two

742   sets of measures were very significantly correlated suggesting that the two labels

743   identify the same structure.

744   In males with a T implant in POM, analysis of the relationship between HVC

745   volume and singing activity had suggested that the increased volume is in part

746   activity-dependent, although local actions of T also participate to the increase in HVC

747   volume as observed in birds which additionally had a T implant near HVC (Alward et

748   al., 2016). Since the amount of T implanted here was similar to the amount implanted

749   in the published male experiments, it can be suspected that the singing activity

750   induced here in females was not intense enough to promote a detectable growth of

751   HVC. Accordingly in this experiment, in contrast to what was observed before in

752   males, no correlation was detected between the number of songs or percentage time

753   spent singing and the measures of HVC volumes (ipsi- or contralateral side, Nissl-

754   stained or DCX-ir cell group; $-0.270 \leq R \leq 0.034$; $p=0.157$ for the largest negative

755   value, $p \geq 0.812$ otherwise). This growth might alternatively be slower in females than

756   in males and a longer exposure to the steroids may have produced significant effects.

757   Surprisingly, however, a significant increase in multipolar DCX-ir cells was

758   observed in the HVC of T birds, while no difference was detected ventral or lateral to

759   HVC. These cellular changes were obviously not sufficient to modify the overall

760   volume of HVC, but they clearly demonstrate that steroid implantation in POM

761   affected the dynamics of neurogenesis in a brain area relevant to song control. Given

762 that effects were bilateral, while T or E2 implants were unilateral, these

763 neuroanatomical effects are likely to be activity-dependent although the numbers of

764 multipolar DCX-ir cells in HVC did not correlate with the measures of song that were

765 affected by the treatments, namely the number of songs and the percentage of time

766 spent singing (all p≥0.141). Interestingly also, the effect was limited to HVC and not

767 seen in two adjacent areas thus stressing again that, as observed before (Balthazart

768 et al., 2008), neurogenesis and recruitment of new neurons is controlled in a specific

769 manner within this song control nucleus.

770 Interestingly, although E2 implanted in POM produced nearly identical effects

771 on vocal behavior, this treatment did not affect DCX-ir multipolar cells in HVC. This

772 differential effect of T and E2 might reflect a differential time-course of action so that

773 the new neurons would have been sampled at a different latency after their final

774 mitotic division in T and E2 birds. This difference affecting DCX-ir cells may indeed

775 relate to the fact already discussed before that the maximal effects of T on song were

776 observed on day 14 but only on day 28 in E2 birds. All these data clearly point to the

777 fact that we would need more studies on the time-course of neurogenesis in HVC.

778

779 *Perineuronal nets and PV-ir neurons*

780 Although PNN density and/or total numbers in HVC are increased by systemic T

781 treatment in adult male canaries (Cornez et al., 2017a), no change was detected

782 here after implantation of T or E2 in the POM. The increase of PNN density in HVC

783 has been hypothesized to play a key role in song crystallization of song by stabilizing

784 synaptic connections of specific subsets of neurons (Balmer et al., 2009; Cornez et

785 al., 2018b; Cornez et al., 2017b). However, no study to date has attempted to

786 determine whether this increase in PNN density is due to a direct effect of T on HVC

787 or is, like neurogenesis, driven at least in part by the singing activity itself. Females

788 bearing a T or E2 implant in POM displayed here an increase in vocalizations, but no

789 change in PNN expression. This observation might be construed to conclude that the

790 PNN expression is not activity-dependent, but is rather controlled by a direct action of

791 steroids in HVC. A major limitation to this conclusion is however that the vocal activity

792 induced here by steroids was quite limited both in quantity and quality. The songs

793 produced by these females also never showed the features of crystalized song so

794 that it makes sense that PNN expression was not increased and actually remained at

795 a very low level comparable to what is observed in females not treated with T

796 (Cornez et al., 2017a) and much below what is seen in sexually mature males

797 (Cornez et al., 2018a) or castrated males treated with exogenous testosterone

798 (Cornez et al., 2017a). Additional studies independently manipulating direct action of

799 T in HVC and singing activity would be needed to reach formal conclusions on this

800 question.

801

802 **In conclusion**, the present study indicates that as observed in males, sex steroids

803 increase the motivation to sing in female canaries by acting in the medial preoptic

804 area and they correlatively increase neurogenesis in HVC. However, as observed

805 after systemic treatments with T, female songs do not reach the same level of quality

806 and are not produced as frequently as male songs. Future research should

807 investigate whether longer treatments or treatments with higher doses of T might be

808 able to overcome this sex difference or if it relates to organizational effects of early

809 exposure to sex steroids or even to direct genetic effects independent of gonadal

810 steroid hormone action.

811

812

Variable	T out Mean±SEM (n)	E2 out Mean±SEM (n)	T vs E2 F, p	Days F, p	Interaction F, p
Number of songs D7	27.7±17.6 (4)	122±57 (5)			
D14	37.5±30.8 (4)	83.8±38.9 (5)			
D28	31.7±12.3 (4)	17.0±11.9 (5)	F=1.204, p=0.308	F=1.783, p=0.216	F=1.961, p=0.177
Song duration D7	0.34±0.11 (4)	0.28±0.12 (5)			
D14	0.35±1.12 (4)	0.39±0.10 (5)			
D28	0.44±0.02 (4)	0.28±0.11 (5)	F=0.245, p=0.629	F=0.303, p=0.674	F=0.809, p=0.465
% Time singing D7	0.41±0.22 (4)	1.61±0.77 (5)			
D14	0.53±0.38 (4)	1.13±0.52 (5)			
D28	0.40±0.17 (4)	0.22±0.15 (5)	F=1.123, p=0.324	F=2.013, p=0.187	F=1.792, p=0.203
Max. Frequency D7	3553±328 (3)	4095±239 (3)			
D14	3580±342 (3)	3727±439 (4)			
D28	3972±403 (4)	4176±213 (3)	F=0.189, p=0.678	F=0.682, p=0.484	F=0.519, p=0.614
Bandwidth D7	1104±167 (3)	1885±834 (3)			
D14	1128±97(3)	2156±1185 (4)			
D28	947±141 (4)	1268±329 (3)	F=1.036, p=0.348	F=0.499, p=0.612	F=0.349, p=0.715
Mean entropy D7	2.98±0.21 (3)	3.29±0.39 (3)			
D14	2.85±0.24 (3)	2.93±0.15 (4)			
D28	2.74±0.16 (4)	2.92±0.10 (3)	F=0.524, p=0.496	F=4.037, p=0.128	F=1.875, p=0.245

Variable	T out	E2 out	T vs E2	Ipsi-Contra	Interaction
POM Volume Ipsi	0.06±0.01 (4)	0.02±0.02 (3)	F=3.022, p=0.142	F=0.811, p =0.408	F=0.227, p=0.653
Contra	0.05±0.01 (4)	0.02±0.01 (3)			
HVC Volume Nissl Ipsi	0.10±0.02 (4)	0.14±0.02 (4)	F=0.810, p=0.403	F=0.516, p =0.499	F=1.507, p=0.265
Contra	0.11±0.02 (4)	0.12±0.02 (4)			
HVC Vol. DCX Ipsi	0.11±0.03 (4)	0.10±0.02 (5)	F=0.053, p=0.824	F=1.032, p =0.343	F=0.002, p=0.967
Contra	0.10±0.02 (4)	0.10±0.01 (5)			
Fusif. DCX in HVC Ipsi	86.2±12.3 (4)	56.0±6.9 (5)	F=3.559, p=0.101	F=5.143, p =0.058	F=3.302, p=0.112
Contra	64.5±10.7 (4)	53.6±4.6 (5)			
Multi. DCX in HVC Ipsi	152.0±35.2 (4)	151.4±9.7 (5)	F=0.001, p=0.976	F=1.715, p =0.232	F=0.053, p=0.824
Contra	142.0±30.7 (4)	144.4±8.0 (5)			
Fusif. DCX vtr. HVC Ipsi	11.2±3.1 (4)	7.8±0.8 (5)	F=1.099, p=0.329	F=0.110, p =0.750	F=0.110, p=0.750
Contra	10.0±2.6 (4)	7.8±2.6 (5)			
Multi. DCX vtr. HVC Ipsi	19.0±3.8 (4)	23.0±2.8 (5)	F=1.255, p=0.300	F=0.161, p =0.700	F=0.044, p=0.839
Contra	18.5±2.6 (4)	21.4±2.1 (5)			
Fusif. DCX lat. HVC Ipsi	13.0±3.5 (4)	7.4±0.7 (5)	F=1.848, p=0.216	F=1.401, p =0.275	F=1.043, p=0.341
Contra	13.2±2.5 (4)	10.8±2.4 (5)			
Multi. DCX lat. HVC Ipsi	8.0±1.3 (4)	7.8±1.5 (5)	F=0.369, p=0.562	F=0.123, p =0.736	F=1.332, p=0.286
Contra	6.5±1.0 (4)	8.6±1.3 (5)			
PNN density Ipsi	36.7±7.0 (3)	34.8±20.4 (5)	F=0.070, p=0.800	F=0.835, p =0.396	F=0.072, p=0.796
Contra	58.0±22.1(3)	46.4±22.6 (5)			
PV-ir density Ipsi	106.3±17.1 (3)	116.6±17.6 (5)	F=1.289, p=0.278	F=0.308, p =0.589	F=0.439, p=0.520
Contra	104.0±0.0 (3)	143.0±25.7 (5)			
PV+PNN density Ipsi	6.0±3.5 (3)	7.6±6.4 (5)	F=0.003, p=0.957	F=0.618, p =0.462	F=0.059, p=0.815
Contra	11.3±3.9 (3)	10.4±4.6 (5)			
% PNN with PV Ipsi	21.3±14.9 (3)	2.2±2.2 (5)	F=0.006, p=0.938	F=1.744, p =0.213	F=1.537, p=0.238
Contra	22.7±5.4 (3)	44.4±23.1 (5)			

813
814 **Table 1.** Mean ± SEM and number of observations for each separate set of OUT data (T and E2 birds),
815 and results of the two-way ANOVAs of these data (F and associated probabilities).
816

817

Figure legends

819

Figure 1: Semi-schematic maps illustrating the implant locations and their content. Panels A through D are presented in a rostral to caudal order. The inset shows the content of the implants (T or E2) and whether they were considered to be located in or out of POM. One E2 implant associated with an asterisk was considered in POM, but was located in a plane caudal to the plane illustrated in D. Panels E and F present photomicrographs of two brain sections immunostained for aromatase, one with an implant outside (dorsal) to POM (E) and one with an implant within the boundaries of the nucleus (F). The asterisk indicates the tip of the implant and the magnification bar is 1 mm in both cases. The induction of aromatase in the POM by T is clearly visible at the tip of the implant in F. Abbreviations-III: third nerve (nervus oculomotorius); CoA: commissura anterior; DSD: decussatio supraoptica dorsalis; DSV: decussatio supraoptica ventralis; GLV: nucleus geniculatus lateralis, pars ventralis; LA: nucleus lateralis anterior thalami; POM: medial preoptic nucleus (nucleus preopticus medialis); Rt: nucleus rotundus; TSM: tractus septopallio-mesencephalicus.

Figure Contributions: Laura Vandries, Samar Ghorbanpoor and Gilles Cornez performed the experiment, Laura Vandries and Jacques Balthazart analyzed the data.

837

Figure 2: Mean ± SEM of all morphological measures collected in the 3 groups of females at the end of the experiment. No significant difference could be detected among the 3 groups except for syrinx mass, but this difference disappears when two

outliers in the Out group are removed (Hatched bar; see text). The number of available data points is indicated in each case at the bottom of the corresponding bar.

Figure Contributions: Laura Vandries, Samar Ghorbanpoor, Gilles Cornez and Olesya Shevchouk performed the experiment, Laura Vandries and Jacques Balthazart analyzed the data.

Figure 3: Representative sonograms illustrating the songs produced by females treated with T or E2 implanted in or out of POM. Birds in the Out group only produced very short songs, usually consisting in the repetition of a single syllable (panels A, B). E2 (panels C-E) or T (panels F-H) implanted in POM increased the duration of some but not all songs that consisted in some cases of multiple syllables. Panel H illustrate one of the most complex songs seen in the T in POM groups.

Figure Contributions: Laura Vandries, Gilles Cornez and Jacques Balthazart analyzed the data.

Figure 4: Summary of all measures of songs produced during 2 hours of recording on days (d) 7, 14 and 28 after implantation of the steroids in the brain. Data were analyzed by two-way ANOVA with the 3 groups as independent factor and the 3 recording days as repeated factor and the results are schematically reported above each graph (Trt= treatment; Time= time after implantation, Int= Interaction; $*=p<0.05$). Significant effects were followed by post hoc Tukey tests whose results are indicated by letters above the bars (a=$p<0.05$ compared to the corresponding Out group). The asterisk above a bar refers to time effects and indicates a significant difference with the D7 point. The number of available data points is indicated in each case at the bottom of the corresponding bar.

866 *Figure Contributions: Laura Vandries and Jacques Balthazart analyzed the data.*

867

868 **Figure 5:** Mean (± SEM) volumes of the POM as identified by the dense cluster of

869 aromatase-immunoreactive cells (A), and of nucleus HVC as identified in Nissl-

870 stained sections (B) and by the dense cluster of doublecortin (DCX)-immunoreactive

871 cells (C) in females treated with T or E2 implanted in or out of POM on the ipsi (left

872 bar in each pair) or contra (right bar in each pair) lateral side. Data were analyzed by

873 two-way ANOVA with the 3 groups as independent and the 2 sides of the brain as

874 repeated factor and the results are schematically reported above each graph (TRT=

875 treatment; SIDE= brain side with respect to the implant, INT= Interaction; **=$p<0.01$,

876 ***=$p<0.001$). Results of Tukey post hoc tests comparing the 3 groups on each brain

877 side are indicated by letters (a, b= $p<0.05$ compared to the Out and E2 group

878 respectively on the same brain side). The number of available data points is indicated

879 in each case at the bottom of the corresponding bar.

880 *Figure Contributions: Laura Vandries, Samar Ghorbanpoor, and Olesya Shevchouk*

881 *performed the experiment, Laura Vandries and Jacques Balthazart analyzed the data.*

882

883 **Figure 6:** Representative photomicrographs of the preoptic area (A, B) or of the song

884 control nucleus HVC (C, D) illustrating the main experimental effects. Panels in the

885 top row show the preoptic area stained for aromatase in a female with a T implant on

886 the right side showing the aromatase induction (A) or in a female of the Out group

887 showing basal aromatase expression (B). Panels in the bottom row show nucleus

888 HVC stained for doublecortin in a female with a T implant in POM (C) and an Out bird

889 (D) illustrating the increase by T in POM of the density of DCX-ir cells in HVC.

890 Magnification bars are 500 µm in both cases and refer to both panels on the same

891 row.

892 *Figure Contributions: Laura Vandries and Samar Ghorbanpoor performed the*

893 *experiment, Laura Vandries and Jacques Balthazart analyzed the data.*

894

895 **Figure 7:** Correlation between the volumes of HVC as measured in Nissl-stained

896 sections (B) and by the dense cluster of doublecortin (DCX)-immunoreactive cells.

897 Data were separately analyzed for volumes measured on the side ipsi- or contra-

898 lateral side to the steroid implants. The graph illustrates the significant regression line

899 and the 95% confidence intervals.

900 *Figure Contributions: Laura Vandries and Jacques Balthazart analyzed the data.*

901

902 **Figure 8:** Mean (± SEM) densities (numbers/mm^3) of fusiform (A, C, E) and

903 multipolar (B, D, F) DCX-ir cells in HVC (A, B) and in area directly ventral (C, D) or

904 lateral (E, F) to this nucleus in the 3 experimental groups on the brain side ipsi- and

905 contra-lateral to the steroid implants. Data were analyzed by two-way ANOVA with

906 the 3 groups as independent and the 2 sides of the brain as repeated factor and the

907 results are schematically reported above each graph (TRT= treatment; SIDE= brain

908 side relative to implant, INT= Interaction; *=p<0.05). Significant effects of treatments

909 were followed by Tukey post-hoc tests whose results are expressed as follows: b=

910 p<0.05 by comparison with the E2 group. The number of available data points is

911 indicated in each case at the bottom of the corresponding bar.

912 *Figure Contributions: Laura Vandries, Samar Ghorbanpoor and Olesya Shevchouk*

913 *performed the experiment, Laura Vandries and Jacques Balthazart analyzed the data.*

914

915 **Figure 9:** Mean (± SEM) densities (numbers/mm^3) of PNN (A), of PV-ir cells (B), of

916 PV-ir cells surrounded by PNN (C) and percentage of PNN present around PV-ir cells

917 (D) in the 3 experimental groups on the side ipsi- and contra-lateral side to the

918 steroid implants. Data were analyzed by two-way ANOVA with the 3 groups as

919 independent and the 2 sides of the brain as repeated factor and the results are

920 schematically reported above each graph (TRT= treatment; SIDE= brain side relative

921 to implant, INT= Interaction). No significant effect was detected. The number of

922 available data points is indicated in each case at the bottom of the corresponding bar.

923 *Figure Contributions: Laura Vandries and Gilles Cornez performed the experiment,*

924 *Laura Vandries and Jacques Balthazart analyzed the data.*

925

926

927

928

References
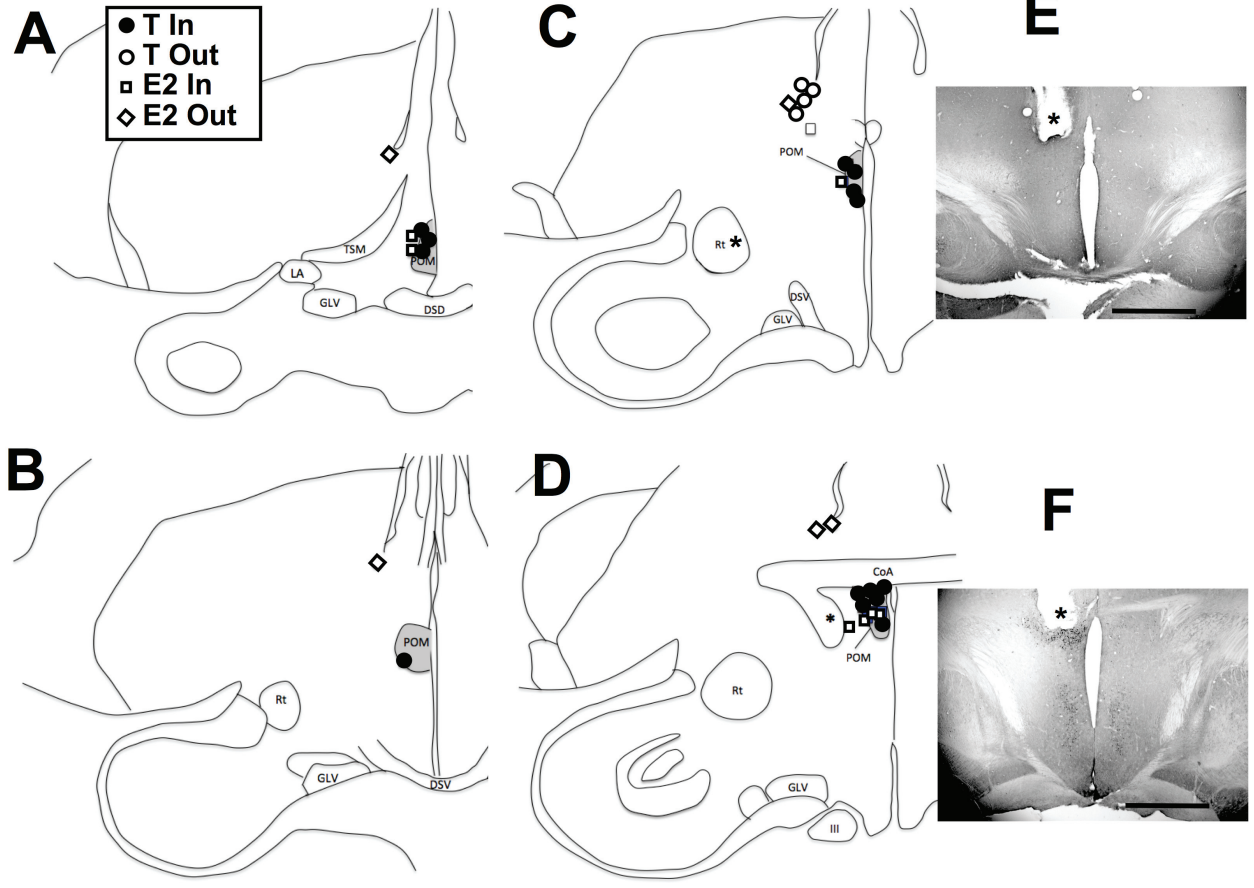
930

Alward, BA, Balthazart, J, Ball, GF, (2013) Differential effects of global versus local testosterone on singing behavior and its underlying neural substrate. Proc Nat Acad Sci USA 110: 19573-19578.

Alward, BA, Balthazart, J, Ball, GF, (2017a) Dissociable Effects on Birdsong of Androgen Signaling in Cortex-Like Brain Regions of Canaries. J Neurosci 37: 8612-8624.

Alward, BA, Madison, FN, Parker, SE, Balthazart, J, Ball, GF, (2016) Pleiotropic Control by Testosterone of a Learned Vocal Behavior and Its Underlying Neuroplasticity. eNeuro 3.

Alward, BA, Mayes, WD, Peng, K, Stevenson, TJ, Balthazart, J, Ball, GF, (2014) Dissociable effects of social context on song and doublecortin immunoreactivity in male canaries. Eur J Neurosci 40: 2941-2947.

Alward, BA, Rouse, ML, Balthazart, J, Ball, GF, (2017b) Testosterone regulates birdsong in an anatomically specific manner. Anim Behavi 124: 291-298.

Ball, GF, (2016) Species variation in the degree of sex differences in brain and behaviour related to birdsong: adaptations and constraints. Phil Trans Roy Soc London Series B, Biological sciences 371: 20150117.

Ball, GF, Riters, LV, MacDougall-Shackleton, SA, Balthazart, J, 2008. Sex differences in brain and behavior and the neuroendocrine control of the motivation to sing, in: Zeigler, H P, Marler, P (Eds.), Neuroscience of birdsong. Cambridge, Cambridge, pp. 320-331.

Balmer, TS, Carels, VM, Frisch, JL, Nick, TA, (2009) Modulation of perineuronal nets and parvalbumin with developmental song learning. J Neurosci 29: 12878-12885.

Balthazart, J, Absil, P, Foidart, A, Houbart, M, Harada, N, Ball, GF, (1996) Distribution of aromatase-immunoreactive cells in the forebrain of zebra finches (Taeniopygia guttata): Implications for the neural action of steroids and nuclear definition in the avian hypothalamus. J Neurobiol 31: 129-148.

Balthazart, J, Absil, P, Viglietti-Panzica, C, Panzica, GC, (1997) Vasotocinergic innervation of areas containing aromatase-immunoreactive cells in the quail forebrain. J Neurobiol 33: 45-60.

Balthazart, J, Ball, GF, (2014) Endogenous versus exogenous markers of adult neurogenesis in canaries and other birds: advantages and disadvantages. J Comp Neurol 522: 4100-4120.
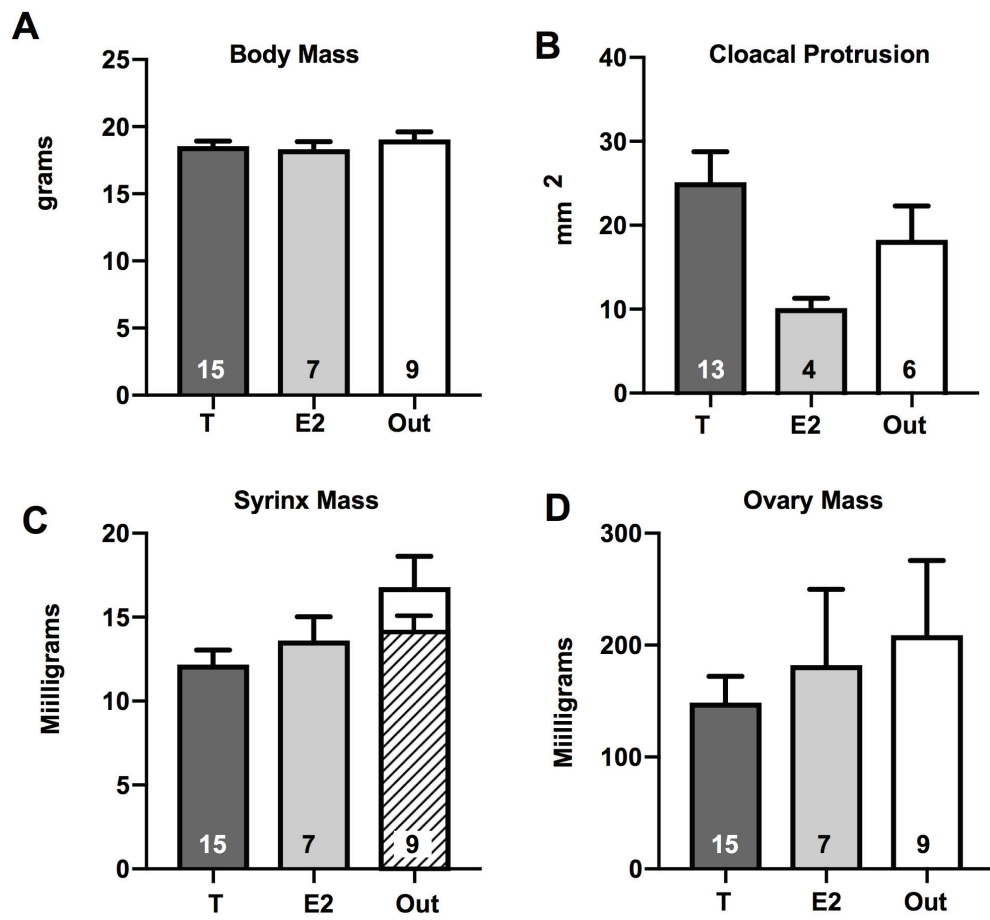
958   Balthazart, J, Boseret, G, Konkle, AT, Hurley, LL, Ball, GF, (2008) Doublecortin as a marker of adult
959   neuroplasticity in the canary song control nucleus HVC. Eur J Neurosci 27: 801-817.

960   Boseret, G, Ball, GF, Balthazart, J, (2007) The microtubule-associated protein doublecortin is broadly
961   expressed in the telencephalon of adult canaries. J Chem Neuroanat 33: 140-154.

962   Catchpole, CK, Slater, PJB, 2008. Bird song. Biological themes and Variations. Cambridge University
963   Press, Cambridge UK.

964   Charlier, TD, Ball, GF, Balthazart, J, (2008) Rapid action on neuroplasticity precedes behavioral
965   activation by testosterone. Horm Behav 54: 488-495.

966   Collins, S, 2004. Vocal fighting and flirting: the functions of birdsong, in: Marler, P, Slabbekoorn, H
967   (Eds.), Nature's Lusic, The Science of Birdsong. Elsevier, Amsterdam, pp. 39-79.

968   Cornez, G, Collignon, C, Müller, W, Ball, GF, Cornil, CA, Balthazart, J, (2018a) Correlation between
969   song learning and perineuronal nets development in song control nuclei of juvenile canaries.
970   Abst Soc Neurosc Meeting San Diego CA 40603/RR3.

971   Cornez, G, Jonckers, E, Ter Haar, SM, Shevchouk, OT, Ghorbanpoor, S, Ball, GF, Van Der Linden, A,
972   Cornil, CA, Balthazart, J, (2017a) Perineuronal nets development correlates with developmental
973   and adult neuroplasticity related to song learning in the songbird brain. Abst Soc Neurosci
974   Washington DC 31806/HH23

975   Cornez, G, Jonckers, E, Ter Haar, SM, Van der Linden, A, Cornil, CA, Balthazart, J, (2018b) Timing of
976   perineuronal net development in the zebra finch song control system correlates with
977   developmental song learning. Proc Roy Soc B 285: DOI: 10.1098/rspb.2018.0849.

978   Cornez, G, Madison, FN, Van der Linden, A, Cornil, C, Yoder, KM, Ball, GF, Balthazart, J, (2017b)
979   Perineuronal nets and vocal plasticity in songbirds: A proposed mechanism to explain the
980   difference between closed-ended and open-ended learning. Dev Neurobiol 77: 975-994.

981   Cornez, G, ter Haar, SM, Cornil, CA, Balthazart, J, (2015) Anatomically discrete sex differences in
982   neuroplasticity in zebra finches as reflected by perineuronal nets. PloS one 10: e0123199.

983   Foidart, A, Reid, J, Absil, P, Yoshimura, N, Harada, N, Balthazart, J, (1995) Critical re-examination of
984   the distribution of aromatase-immunoreactive cells in the quail forebrain using antibodies raised
985   against human placental aromatase and against the recombinant quail, mouse or human
986   enzyme. J Chem Neuroanat 8: 267-282.

987   Fusani, L, Gahr, M, (2006) Hormonal influence on song structure and organization: the role of
988   estrogen. Neuroscience 138: 939-946.

989   Fusani, L, Metzdorf, R, Hutchison, JB, Gahr, M, (2003) Aromatase inhibition affects testosterone-
990   induced masculinization of song and the neural song system in female canaries. J Neurobiol 54:
991   370-379.

992   Fusani, L, Van't Hof, T, Hutchison, JB, Gahr, M, (2000) Seasonal expression of androgen receptors,
993   estrogen receptors, and aromatase in the canary brain in relation to circulating androgens and
994   estrogens. J Neurobiol 43: 254-268.

995   Gahr, M, Metzdorf, R, Schmidl, D, Wickler, W, (2008) Bi-directional sexual dimorphisms of the song
996   control nucleus HVC in a songbird with unison song. PloS one 3: e3073.

997   Gentner, TQ, Hulse, SH, (2000) Female European starling preference and choice for variation in
998   conspecific male song. Anim Behav 59: 443-458.

999   Harada, N, Abe-Dohmae, S, Loeffen, R, Foidart, A, Balthazart, J, (1993) Synergism between
1000   androgens and estrogens in the induction of aromatase and its messenger RNA in the brain.
1001   Brain Res 622: 243-256.

1002   Harding, CF, 2008. Hormonal modulation of singing behavior: methodology and principles of hormone
1003   action, in: Zeigler, H P, Marler, P (Eds.), Neuroscience of birdsong. Cambridge University Press,
1004   Cambridge, pp. 305-319.

1005   Hartog, TE, Dittrich, F, Pieneman, AW, Jansen, RF, Frankl-Vilches, C, Lessmann, V, Lilliehook, C,
1006   Goldman, SA, Gahr, M, (2009) Brain-derived neurotrophic factor signaling in the HVC is
1007   required for testosterone-induced song of female canaries. J Neurosci 29: 15511-15519.

1008   Hurley, LL, Wallace, AM, Sartor, JJ, Ball, GF, (2008) Photoperiodic induced changes in reproductive
1009   state of border canaries (Serinus canaria) are associated with marked variation in hypothalamic
1010   gonadotropin-releasing hormone immunoreactivity and the volume of song control regions. Gen
1011   Comp Endocrinol 158: 10-19.

1012   Hutchison, JB, Joris, S, Hutchison, RE, Steimer, T, (1989) Steroid control of sexual behavior and brain
1013   aromatase in the dove: Effects of nonaromatizable androgens, methyltrienolone (R1881), and
1014   5alpha-dihydrotestosterone. Horm Behav 23: 542-555.

1015   Hutchison, JB, Steimer, TH, (1986) Formation of behaviorally effective 17beta-estradiol in the dove
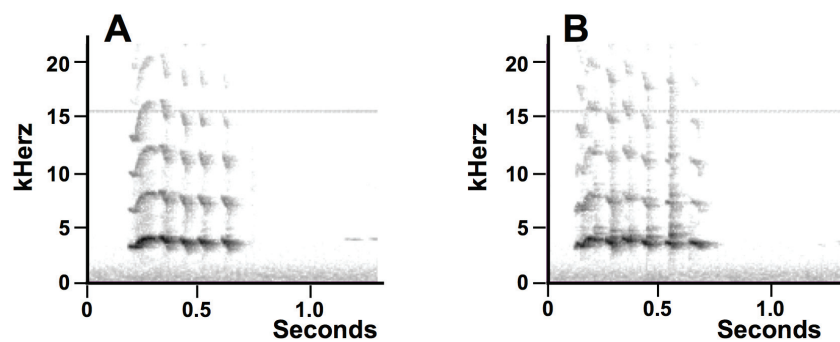1016   brain: steroid control of preoptic aromatase. Endocrinology 118: 2180-2187.

1017   Luine, V, Nottebohm, F, Harding, CF, McEwen, BS, (1980) Androgen affects cholinergic enzymes in
1018   syringeal motor neurons and muscles. Brain Res 192: 89-107.

1019   MacDougall-Shackleton, SA, Ball, GF, (1999) Comparative studies of sex differences in the song-
1020   control system of songbirds. Trends in Neurosciences 22: 432-436.

1021   Madison, FN, Rouse, ML, Jr., Balthazart, J, Ball, GF, (2015) Reversing song behavior phenotype:
1022   Testosterone driven induction of singing and measures of song quality in adult male and female
1023   canaries (Serinus canaria). Gen Comp Endocrinol 215: 61-75.

1024   Metzdorf, R, Gahr, M, Fusani, L, (1999) Distribution of aromatase, estrogen receptor, and androgen
1025   receptor mRNA in the forebrain of songbirds and nonsongbirds. J Comp Neurol 407: 115-129.

1026   Nottebohm, F, (1980) Testosterone triggers growth of brain vocal control nuclei in adult female
1027   canaries. Brain Res 189: 429-436.

1028   Nottebohm, F, Arnold, AP, (1976) Sexual dimorphism in the vocal control areas in the song bird brain.
1029   Science 194: 211-213.

1030   Nottebohm, F, Nottebohm, M.E., Crane, L, (1986) Developmental and seasonal changes in canary
1031   song and their relation to changes in the anatomy of song-control nuclei. Behav Neural Biol 46:
1032   445-471.

1033   Nottebohm, F, Nottebohm, ME, Crane, LA, Wingfield, JC, (1987) Seasonal changes in gonadal
1034   hormone levels of adult male canaries and their relation to song. Behav Neural Biol 47: 197-211.

1035   Nowicki, S, Searcy, WA, (2014) The evolution of vocal learning. Current Opinion Neurobiol 28: 48-53.

1036   Odom, KJ, Benedict, L, (2018) A call to document female bird songs: Applications for diverse fields.
1037   The Auk 135: 314-325.

1038   Odom, KJ, Hall, ML, Riebel, K, Omland, KE, Langmore, NE, (2014) Female song is widespread and
1039   ancestral in songbirds. Nature Comm 5: 3379.

1040   Saldanha, CJ, Tuerk, MJ, Kim, YH, Fernandes, AO, Arnold, AP, Schlinger, BA, (2000) Distribution and
1041   regulation of telencephalic aromatase expression in the zebra finch revealed with a specific
1042   antibody. J Comp Neurol 423: 619-630.

1043   Schlinger, BA, Brenowitz, EA, 2017. Neural and hormonal control of birdsong, in: Pfaff, D W, Joels, M
1044   (Eds.), Hormones, brain and behavior, 3rd ed. Academic Press, Oxford, pp. 255-290.

1045   Shevchouk, OT, Ball, GF, Cornil, CA, Balthazart, J, (2017a) Studies of HVC Plasticity in Adult
1046   Canaries Reveal Social Effects and Sex Differences as Well as Limitations of Multiple Markers
1047   Available to Assess Adult Neurogenesis. PloS one 12: e0170938.

1048   Shevchouk, OT, Ball, GF, Cornil, CA, Balthazart, J, (2019) Rapid testosterone-induced growth of the
1049   medial preoptic nucleus in male canaries. Physiol. Behav. 204 :20-26

1050   Shevchouk, OT, Ghorbanpoor, S, Ball, GF, Cornil, CA, Balthazart, J, (2017b) Testosterone-induced
1051   neuroendocrine changes in the medial preoptic area precede song activation and plasticity in
1052   song control nuclei of female canaries. Eur J Neurosci 45: 886-900.

1053   Shevchouk, OT, Ghorbanpoor, S, Smith, E, Liere, P, Schumacher, M, Ball, GF, Cornil, CA, Balthazart,
1054   J, (2018b) Behavioral evidence for sex steroids hypersensitivity in castrated male canaries.
1055   Horm Behav 103: 80-96.

1056   Stokes, TM, Leonard, CM, Nottebohm, F, (1974) The telencephalon, diencephalon, and
1057   mesencephalon of the canary, Serinus canaria, in stereotaxic coordinates. J Comp Neurol 156:
1058   337-374.

1059   Tramontin, AD, Hartman, VN, Brenowitz, EA, (2000) Breeding conditions induce rapid and sequential
1060   growth in adult avian song control circuits: A model of seasonal plasticity in the brain. J
1061   Neurosci 20: 854-861.

1062   van 't Spijker, HM, Kwok, JCF, (2017) A Sweet Talk: The Molecular Systems of Perineuronal Nets in
1063   Controlling Neuronal Communication. Fron Integrative Neurosci 11: 33.

1064   Yamamura, T, Barker, JM, Balthazart, J, Ball, GF, (2011) Androgens and estrogens synergistically
1065   regulate the expression of doublecortin and enhance neuronal recruitment in the song system of
1066   adult female canaries. J Neurosci 31: 9649-9657.

1067

A

● T In
○ T Out
□ E2 In
◇ E2 Out

TSM
LA
GLV
POM
DSD

B

Rt
POM
GLV
DSV

C

POM
Rt *
DSV
GLV

D

CoA
*
POM
Rt
GLV
III

E

F

A Body Mass

grams

25
20
15
10
5
0

15   7   9

T   E2   Out

B Cloacal Protrusion

mm 2

40
30
20
10
0

13   4   6

T   E2   Out

C Syrinx Mass

Miilligrams

20
15
10
5
0

15   7   9

T   E2   Out

D Ovary Mass
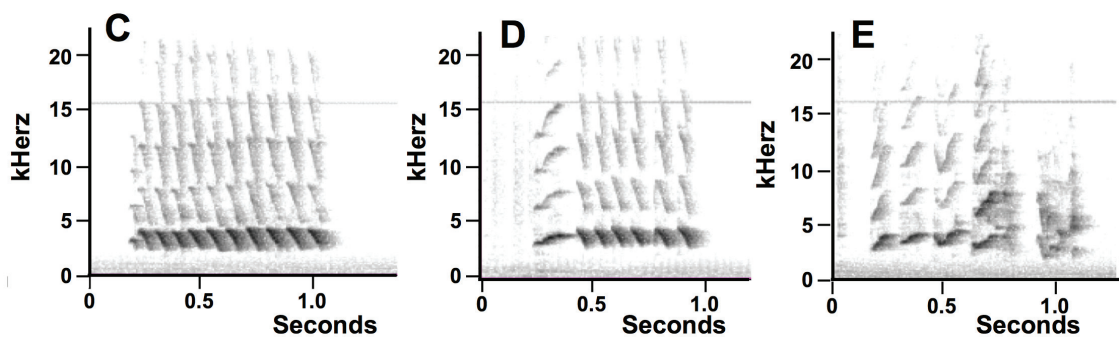
Miilligrams

300
200
100
0

15   7   9

T   E2   Out

Out group

E2 in POM group

T in POM group

A Number of songs

B Song duration

C Percent time singing

D Maximum frequency

E Bandwidth 90%

F Average Entropy

Legend: T (black), E2 (gray), Out (white)

A

Ipsilateral side

B

Contralateral side

IN HVC

A Fusiform DCX cells density

B Multipolar DCX cells density

VENTRAL TO HVC

C Fusiform DCX cells density

D Multipolar DCX cells density

LATERAL TO HVC

E Fusiform DCX cells density

F Multipolar DCX cells density